

Lorentz contraction, geometry and range in antiproton-proton annihilation into two pions

Bruno El-Bennich* and W.M. Kloet†

*Laboratoire de Physique Nucléaire et de Hautes Énergies, Theory Group,
Université Pierre et Marie Curie, Paris, France

† Department of Physics and Astronomy, Rutgers University, Piscataway, New Jersey, USA

Abstract.

We present a geometric interpretation of the so-called annihilation range in reactions of the type $\bar{p}p \rightarrow$ two light mesons based upon Lorentz effects in the highly relativistic final states ($\gamma = E_{\text{cm}}/2mc^2 \simeq 6.8 - 8.0$). Lorentz-boosted meson wave functions, within the framework of the constituent quark model, result in a richer angular dependence of the annihilation amplitudes and thus in higher partial wave contributions ($J > 1$) than usually obtained. This approach sheds some light on what could be a "short" annihilation range and how it is influenced by the angular distribution of the final states.

In this talk we summarize the results obtained in Refs. [1–3] while focusing on the details of Lorentz effects in reactions of the type $\bar{p}p \rightarrow \pi^- \pi^+$ or $\bar{p}p \rightarrow K^- K^+$ when the final states are highly energetic. The initial motivation is twofold: for one, a long-standing debate about the antiproton-proton range exists in which proponents of a very short annihilation range, of the order of the Compton wavelength of the annihilating baryons ($r_{\text{ann.}} = m_N^{-1} \simeq 0.1$ fm), emphasize the role of analytical properties of Feynman graphs [4]. This should be *a priori* the range of baryon exchange in the t -channel.

Comparison of baryon exchange model results [5–8] with $\bar{p}p \rightarrow \pi^- \pi^+$ and $\bar{p}p \rightarrow K^- K^+$ data on differential cross sections $d\sigma/d\Omega$ and analyzing powers A_{0n} , as measured in the pre-LEAR experiments at CERN and KEK [9–11] as well as at LEAR [12], nonetheless clearly indicates that these models are too short ranged. They give vanishing total $\bar{p}p$ angular momentum $J \geq 1$ contributions to the annihilation amplitudes, whereas partial wave analyzes [13–16] of both the pre-LEAR [9–11] and LEAR [12] data consistently point to higher partial wave amplitudes with J up to 3 or 4. Of course, compared with elastic proton-proton scattering, where partial waves up to $J = 9 - 10$ are necessary to fit the data, antiproton-proton annihilation is a short-range interaction. Yet, the experiments mentioned above seem not to confirm the *extreme* shortness implied by the baryon exchange models. It is worthwhile to note that the annihilation range is not merely given by the Compton wavelength of the baryons alone. In general, the annihilation vertices are regularized with appropriate form factors, which smear out the baryon-meson interaction. For example, in the case of Ref. [8] the form factor of the pseudovector pion-proton coupling is found to improve the fits to $\bar{p}p \rightarrow \pi^- \pi^+$ cross sections and analyzing powers. It is therefore not advisable to ascribe the annihilation range solely to heavy baryon exchange in the t -channel.

The use of alternative geometric arguments, such as the minimal overlap for annihilation of an $\bar{p}p$ pair within a quark picture motivated by bag models, was investigated by Alberg *et al.* [17]. In their fit to $\bar{p}p$ scattering data the effective nucleon bag radius R takes on values of 0.6 – 1.1 fm. The crucial assumption is that $\bar{p}p$ annihilation proceeds only when the \bar{p} and p bags overlap so the quarks and antiquarks can rearrange or annihilate to form the observed mesons. In Ref. [17] the annihilation is found to peak at 0.7 fm or 0.95 fm depending on the bag-model form used. Hence, in geometric terms the annihilation range is roughly twice the nucleon radius which is much larger than the Compton wavelength of the nucleon. If one uses a chiral bag model then the pressure of the mesonic cloud about the core quarks decreases the nucleon bag radius. Since the external mesons are not believed to participate in the $\bar{p}p$ annihilation, the upper bound for the annihilation range is somewhat lowered. Nonetheless, quark model calculations also fail to reproduce the LEAR data [18, 19] as they too are rather short-ranged. The range, in this case, is an intrinsic property of overlap integrals involving (anti)quark wavefunctions with size parameters that reproduce the particle radii known from fits as the one just mentioned [17].

Yet another approach to define an annihilation range is due to Povh and Walcher [20] and was subsequently applied by the Bonn group [21] to the Bonn and Paris $\bar{N}N$ potentials. In a nutshell, the method consists of taking the quantity $p_l(r) = 2/\hbar W_{\bar{N}N} R_l^*(r) R_l(r) r^2$ as the annihilation probability for a partial wave of angular momentum l , where $R_l(r)$ is the radial component of the (Bonn or Paris) $\bar{N}N$ wavefunction and $W_{\bar{N}N}$ the imaginary part of the potential. Plotting $p_l(r)$ for several partial waves, they found for the Paris $\bar{N}N$ potential a maximum localized at about 0.5 fm and for the Bonn $\bar{N}N$ potential this value is about 1.1 fm. This range compares well with the quark model prediction discussed in the previous paragraph.

The second motivation stems from the observation that the Hasan *et al.* LEAR data [12] reveals a strong left-right asymmetry with respect to the beam direction and displays large variations of the cross sections as a function of the c.m. angle. In our work, we try to determine how relativistic effects, namely Lorentz contractions in quark-model wavefunctions, influence the annihilation amplitudes and whether these effects are relevant to the annihilation range.

QUARK MODEL AND INTRINSIC MESON WAVEFUNCTIONS

In a quark model description of the $\bar{p}p$ annihilation process, one usually seeks guidance from Feynman diagrams in order to deduce appropriate transition operators (*i.e.* the operators linking the initial $\bar{p}p$ quarks and antiquarks so they form the right $\bar{q}q$ pairs). These so-called quark-line diagrams (QLD) are classified according to their flavor-flux topology into rearrangement or annihilation diagrams. In the former case a $\bar{q}q$ pair is annihilated and a quark and antiquark are rearranged to produce the final mesons, while in the latter case two $\bar{q}q$ pairs are annihilated and an $\bar{q}q$ state is created in the final state. The $\bar{q}q$ pairs annihilate into states with distinct quantum numbers J^P and I . In a way, one can conceive of the model as an expansion of the annihilation amplitude in terms of increasing total angular momentum J^P . Parity requires the $\bar{q}q$ pairs be annihilated/created in an $S = 1$ state. Thus the spin-multiplicity is fixed and for

$J^P = 0^+, 1^- \dots$ one gets ${}^3P_0, {}^3S_1 \dots$ annihilation operators. For a concise review of the QLD see, for instance, Ref. [22]. The resulting transition operators may be written in a Hamiltonian form for both the 3P_0 and 3S_1 cases as

$$\begin{aligned} \mathcal{H}({}^3P_0) &= \gamma \sum_{ijmn} a_m^\dagger(\mathbf{k}') a_n(\mathbf{k}) a_i(\mathbf{p}) b_j(\mathbf{p}') \boldsymbol{\sigma} \cdot (\mathbf{p} - \mathbf{p}') (2\pi)^3 \delta(\mathbf{k}' - \mathbf{k} - \mathbf{p}' - \mathbf{p}) + \text{h.c.} \quad (1) \\ \mathcal{H}({}^3S_1) &= \kappa \sum_{ijmn} a_m^\dagger(\mathbf{k}') a_n(\mathbf{k}) a_i(\mathbf{p}) b_j(\mathbf{p}') \left[-2 \boldsymbol{\sigma}_{ij} \cdot \mathbf{k} + i (\boldsymbol{\sigma}_{mn} \times \boldsymbol{\sigma}_{ij}) \cdot (\mathbf{k} - \mathbf{k}') \right] \times \\ &\quad \times (2\pi)^3 \delta(\mathbf{k}' - \mathbf{k} - \mathbf{p}' - \mathbf{p}) + \text{h.c.}, \quad (2) \end{aligned}$$

where color indices have been suppressed and $ijmn$ sums over flavor states. The delta-function imposes momentum transfer from the annihilated $\bar{q}q$ pair to one of the remaining (anti)quarks. Additionally, color is exchanged in the 3S_1 mechanism since $J^P = 1^-$ is the quantum number of the gluon. The relative strength $\lambda = |\gamma/\kappa|$ is a fit parameter.

Confinement is simulated in a harmonic oscillator basis. The single (anti)quark wavefunctions are therefore bundled in Gaussian wave packets in which the c.m. motion of the (anti)proton and pions can be separated from the relative motion of their respective quarks and antiquarks. The total wavefunction of the pion, for example, writes in momentum space as

$$\phi_\pi(\mathbf{p}_i, \mathbf{p}_j) = N_\pi \left(\frac{4\pi}{\beta} \right)^{3/2} u(\mathbf{p}_i) v(\mathbf{p}_j) \chi_{\text{iso}} \chi_{\text{color}} \exp \left\{ -\frac{1}{2\beta} \sum_{\mu=i,j} \left[\mathbf{p}_\mu - \frac{1}{2} \mathbf{Q}_\pi \right]^2 \right\}. \quad (3)$$

Here, \mathbf{p}_i and \mathbf{p}_j are the $\bar{q}q$ momenta and $\mathbf{Q}_\pi = \mathbf{p}_i + \mathbf{p}_j$ is the pion momentum in the c.m. frame whereas $u(\mathbf{p}_i)$ and $v(\mathbf{p}_j)$ are the usual quark and antiquark Dirac spinors. The size parameter β is chosen so as to give the pion a radius $r_\pi = 0.48$ fm.

LORENTZ EFFECTS IN FINAL STATES

So far, we have dealt with the wave representation of the pion in its rest frame where it is spherical (meson in an s -wave). In $\bar{p}p \rightarrow \pi^- \pi^+$, on the other hand, the pions are produced at considerable c.m. energies already at very low \bar{p} -beam energies ($\sqrt{s} = 1.9 - 2.2$ GeV in Ref. [12]). The large mass difference between the pion and the proton causes the final state to be highly relativistic, as can be simply seen from the relativistic factor $\gamma = \sqrt{s}/2m_\pi c^2 \simeq 6.8 - 8.0$. In computing the annihilation amplitudes (and observables), one puts oneself in the c.m. frame in order to compare with experiment. Therefore, *all* ingredients must be transformed to the c.m. For the pions, this means they are not spherical anymore, since they are boosted from their rest frame to the c.m. frame. Eq. (3) cannot be used as such and instead the general Lorentz transformation $\mathbf{p}'_i \equiv l^{-1} \mathbf{p}_i$ (where \mathbf{p}_i is a quark momentum in the pion rest frame) yields

$$\begin{aligned} \phi_\pi(l^{-1} \mathbf{p}_i, l^{-1} \mathbf{p}_j) &= \frac{N_\pi}{\sqrt{\gamma}} \left(\frac{4\pi}{\beta} \right)^{3/2} d_{\lambda\lambda'}^{1/2}(\theta) u(l^{-1} \mathbf{p}_i, \lambda) d_{\lambda\lambda'}^{1/2}(-\theta) v(l^{-1} \mathbf{p}_j, \lambda) \chi_{\text{iso}} \chi_{\text{color}} \times \\ &\quad \times \exp \left\{ -\frac{1}{4\beta} \left[(\mathbf{p}_i - \mathbf{p}_j)^2 + \left(\frac{1}{\gamma^2} - 1 \right) \left([\mathbf{p}_i - \mathbf{p}_j] \cdot \hat{\mathbf{Q}}_\pi \right)^2 \right] \right\}. \quad (4) \end{aligned}$$

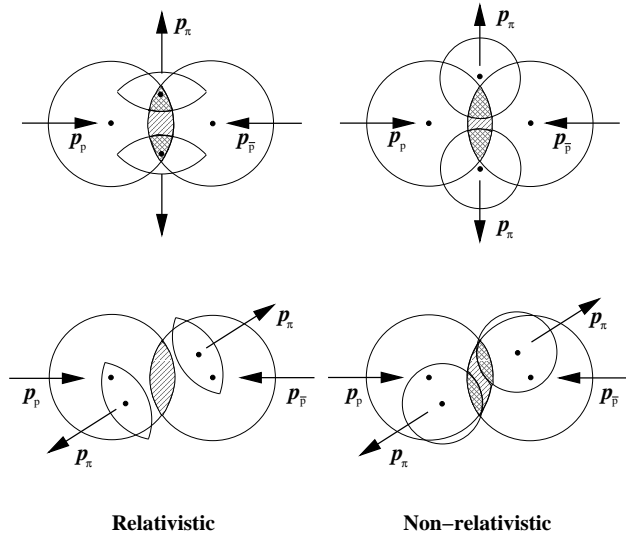


FIGURE 1. Geometry of the overlap in the $\bar{p}p \rightarrow \pi^- \pi^+$ annihilation. See text for details.

In the exponent, the momentum components along the boost direction $\hat{\mathbf{Q}}_\pi = \mathbf{Q}_\pi / |\mathbf{Q}_\pi|$ have been separated from the perpendicular ones. Naturally, for $\gamma = 1$ one retrieves the original wavefunction in Eq. (3). The additional factor $1/\sqrt{\gamma}$ is due to proper normalization to one of the wavefunction. The Lorentz transformations are effected on the Dirac spinors via the Wick rotations $d_{\lambda\lambda'}^{1/2}(\theta)$ in spin space, where the Wick angle θ depends on the relativistic factor $\beta = v/c$ rather than on γ . The indices λ and λ' are the (anti)quark helicities in the pion rest frame and in the c.m. frame, respectively. We have applied the c.m. equal-time condition $t'_i = t'_j$ for the time components of the quark and antiquark, which is also frequently used in Bethe-Salpeter approaches. The effect of the time components is currently under investigation. While the boosting of spinors gives rise to subtle interference effects in the annihilation amplitudes (see discussion in Ref. [2]), its magnitude is negligible compared with the γ -components. Once the wavefunctions of Eq. (4) are employed to derive the annihilation amplitudes, it becomes clear that the boost effects are dramatic. In summary, the annihilation amplitudes, being of Gaussian form, acquire new relativistic terms. Their magnitude can be, depending on the γ (and hence \sqrt{s}) value, up to two orders of magnitude larger than the one of non-relativistic terms. Furthermore, this strong γ -dependence is not constant. The boosts also introduce an angular dependence by means of the projection on the boost direction $\hat{\mathbf{Q}}_\pi$ in the exponential. It is this dependence (which at the hadronic level equates to the c.m. angle between the antiproton beam and an outgoing pion) that is novel and crucial to any improvement in a fit to the LEAR data.

ANNIHILATION AND GEOMETRY

In the following, we propose a somewhat different geometric interpretation. The strong modification of both the 3P_0 and 3S_1 annihilation amplitudes is entirely due to the Lorentz

contractions in the pions. In the overlap integrals this implies a narrowed overlap of the initial $\bar{p}p$ pair and the final pion wave functions. At first sight, this looks discouraging since our introductory discussion revolved around how to increase the annihilation range in a quark model. Yet, this decrease in overlap is merely one piece of the puzzle. The other part is illustrated in Fig. 1 where tentatively the angle dependence of the amplitudes due to relativistic effects is shown for two cases. The smaller blobs represent the pions and are round for $\gamma = 1$ and oval (Lorentz contracted) otherwise. The distances between the two pions and the proton and antiproton are the same in each picture. However, in the first case the pions are produced perpendicularly to the \bar{p} beam direction and all particles overlap. They do so somewhat less when the pions are contracted. In the second case, where the pions are emitted at a different angle, the four spheres overlap if relativity is neglected while the two pion-ellipsoids overlap much less with the the $\bar{p}p$ spheres if relativity is included. This angle-dependent overlap is responsible for a richer angular dependence of the annihilation amplitudes. We therefore obtain significant contributions to $J \geq 1$ partial waves not present previously and a fit to the LEAR data [12] is quite successful [3]. On the other hand, it is clear that one cannot define an annihilation range *per se* since this range depends on the pion direction with respect to the initial \bar{p} -beam. Even so, one can conclude that in order for the $\bar{p}p$ pair to annihilate, the quarks and antiquarks must have a considerable overlap whose size is less than two nucleon radii.

ACKNOWLEDGMENTS

We appreciated helpful discussions with Mary Alberg, Thomas Gutsche, Benoît Loiseau, Johann Haidenbauer, Fred Myhrer and Slawomir Wycech.

REFERENCES

1. B. El-Bennich, W.M. Kloet, and B. Loiseau, Phys. Rev. C **68**, 014003 (2003).
2. B. El-Bennich and W.M. Kloet Phys. Rev. C **70**, 034001 (2004).
3. B. El-Bennich and W.M. Kloet Phys. Rev. C **70**, 034002 (2004).
4. See for example I.S. Shapiro or S.J. Brodsky in *Baryon-Antibaryon Nuclear Interactions*, F. Bradamante, J.-M. Richard, R. Klapisch (Eds.), International School of Physics with Low-Energy Antiprotons, Erice, Italy, Plenum Press, New York (1990).
5. B. Moussallam, Nucl. Phys. **A407**, 413 (1983); *ibid.* **A429**, 429 (1984).
6. V. Mull, J. Haidenbauer, T. Hippchen, and K. Holinde, Phys. Rev. C **44**, 1337 (1991).
7. V. Mull, K. Holinde, and J. Speth, Phys. Lett. **B275**, 12 (1992).
8. Y. Yan and R. Tegen, Phys. Rev. **C54**, 1441 (1996); *ibid.* Nucl. Phys. **A648**, 89 (1999).
9. E. Eisenhandler *et al.*, Nucl. Phys. **B96**, 109 (1975).
10. A. A. Carter *et al.*, Nucl. Phys. **B127**, 202 (1977).
11. T. Tanimori *et al.*, Phys. Rev. Lett. **55**:1835–1838, 1985.
12. A. Hasan *et al.*, Nucl. Phys. **B378**, 3 (1992).
13. M. N. Oakden and M. R. Pennington, Nucl. Phys. **A574**, 731 (1994).
14. A. Hasan and D. V. Bugg, Phys. Lett. **B334**, 215 (1994).
15. W. M. Kloet and F. Myhrer, Phys. Rev. **D53**, 6120 (1996); *ibid.* Z. Phys. **A358**, 423 (1997).
16. B. R. Martin and G. C. Oades, Phys. Rev. **C56**, 1114 (1997); *ibid.* Phys. Rev. **C57**, 3492 (1998).
17. M. Alberg *et al.*, Phys. Rev. **D27**, 536 (1983).
18. G. Bathas and W.M. Kloet, Phys. Lett. **B301**, 155 (1993); *ibid.* Phys. Rev. C **47**, 2207 (1993).

19. A. Muhm, T. Gutsche, R. Thierauf, Y. Yan, and A. Faessler, Nucl. Phys. **A598**, 285 (1996).
20. B. Povh and T. Walcher, Comments Nucl. Part. Phys. Vol. **16**, 85 (1986).
21. J. Haidenbauer, T. Hippchen, and K. Hollinde, Nucl. Phys. **A508**, 329 (1990).
22. C.B. Dover, T. Gutsche, M. Maruyama, and A. Faessler, Prog. Part. Nucl. Phys. **29**, 87 (1992).